ORIGINAL ARTICLE

Cytometry
PART A
Journal of the International Society for Advancement of Cytometry

Rapid and Cost-Efficient Enumeration of Rare Cancer Cells from Whole Blood by Low-Loss Centrifugo-Magnetophoretic Purification Under Stopped-Flow Conditions

Daniel Kirby, Macdara Glynn, Gregor Kijanka, Jens Ducrée*

Biomedical Diagnostics Institute, National Centre of Sensor Research, School of Physical Sciences, Dublin City University, Dublin, Ireland

Received 27 March 2014; Revised 5 September 2014; Accepted 17 October 2014

Grant sponsor: Science Foundation Ireland, Grant number: 10/CE/B1821

Grant sponsor: ERDF and Enterprise Ireland, Grant number: CF 2011 1317

Additional Supporting Information may be found in the online version of this article.

*Correspondence to: Jens Ducrée, Dublin City University, School of Physical Sciences, Glasnevin, Dublin 9, Ireland. E-mail: jens.ducree@dcu.ie

Published online 29 October 2014 in Wiley Online Library (wileyonlinelibrary.com)

DOI: 10.1002/cyto.a.22588

Abstract

We present a substantially improved design and functionality of a centrifugo-magnetophoretic platform which integrates direct immunoseparation and cost-efficient, bright-field detection of cancer cells in whole blood. All liquid handling takes place in a disposable cartridge with geometry akin to a conventional compact disc (CD). The instrumentation required to process such a "lab-on-a-disc" cartridge can be as simple and cost-efficient as the rotor on a common optical disc drive. In a first step, target cells in a blood sample are specifically bound to paramagnetic microbeads. The sample is then placed into the disc cartridge and spun. In the second step, magnetically tagged target cells are separated by a co-rotating, essentially lateral magnetic field from the background population of abundant blood cells, and also from unbound magnetic beads. A stream of target cells centrifugally sediments through a stagnant liquid phase into a designated detection chamber. The continuous, multiforce immunoseparation proceeds very gently, i.e. the mechanical and hydrodynamic stress to the target cells is minimized to mitigate the risk of cell loss by collective entrapment in the background cells or vigorous snapping against a wall. We successfully demonstrate the extraction of MCF7 cancer cells at concentrations as low as 1 target cell per μl from a background of whole blood, with capture efficiencies of up to 88%. Its short time-to-answer is a notable characteristic of this system, with 10% of target cells collected in the first minute after their loading to the system and the remainder captured within the following 10 min. All the above-mentioned factors synergetically combine to leverage the development of a prospective point-of-care device for CTC detection.

Key terms

rare cell separation; centrifugal microfluidics; lab-on-a-disc; CTC detection; stopped flow

OVER the past two decades interest in the centrifugal microfluidic lab-on-a-disc (LoaD) concept (1,2) has significantly increased, in particular for bioanalytical assays. The platform has been applied to successfully integrate liquid handling and detection for endpoints such as sample nucleic acid amplification, immunoassays (3), and cell analysis (4,5). The use of the inherent centrifugal field to transport and manipulate (liquid) analytes and reagents (rather than through complex actuation schemes such as pumps) makes the LoaD platforms particularly attractive for point-of-care (PoC) settings where both cost-efficiency and robustness are prerequisites. Processing of the disposable disc-cartridge generally requires a speed-adjustable spindle motor as, for instance, found in conventional DVD players; indeed, such cartridges have previously been processed by the DVD-ROM drive of a laptop (6). Additionally, the innate ability of centrifugal sedimentation makes LoaD platforms particularly suited to blood processing and cell handling.

ISAC
International Society for Advancement of Cytometry

Very dynamically emerging trends of personalised medicine and acute healthcare have underpinned the need for advanced point-of-care (PoC) devices or companion diagnostics which can be deployed at the bedside in hospitals, in doctor's offices, and even at home for patient self-testing. Classically these tests have been carried out in central laboratories, involving long time-to-answer and high costs of instrumentation. Microfluidic platforms bear the promise to enhance patient comfort through fewer visits to clinics and more gentle blood sampling due to reduced volume requirements while alleviating the burden on health-care budgets. A notable example is the large-scale HIV monitoring in resource-poor settings of Sub-Saharan Africa, where a number of microfluidic technologies for rapid, minimum-infrastructure PoC testing and timely initiation of medical intervention. Much of these microtechnologies are based on cell analysis from whole blood samples (7).

In addition to mobile monitoring of disease, these devices have also become a major driver of cell-based medical analysis in clinics and hospitals. A primary objective for such application is in the detection of extremely rare circulating tumour cells (CTCs) in whole blood samples. The field has considerably advanced in recent years (8,9), with a growing number of research groups investigating a range of aspects, from biological characteristics of cancer cells (10) such as the links between CTCs and metastases (11), to instrumentation designed for diagnostics based on counting the actual CTC numbers present in the blood (12), associated prognosis (13), methods of enumerating and detecting CTCs (8,14,15) and research into developing diagnostic devices which are able to detect CTCs in typical clinical settings (9). Tools for CTC detection are expected to provide important, ideally patient-specific information for cancer prognosis, diagnosis, assessment of minimal residual disease, and assessment of anti-cancer drugs (16).

Much effort is directed towards the development of microfluidic systems for detecting CTCs (17–21). The paramount challenge is the extreme sparseness of such cells. While the CTC concentration in a patient sample is known to vary greatly with cancer type and stage (14), the scientific community has not yet been able to define a gold standard experiment for the unambiguous identification of a CTC; hence also a wide consensus on their concentration range is notably lacking. Nevertheless, we here follow the assumption of a concentration in the range of 1 cell per μl. However, note that some work refers to concentrations as low as 1 cell per ml, a concentration which would require an initial enrichment on our current system, for instance implementing RBC lysis or buffy coat extraction. Due to the extreme paucity of these cells, an efficient and reliable diagnostic instrument must meet particular performance criteria: (i) a capture platform must isolate the entire CTC population present (low loss, high capture efficiency), (ii) discard background non-target cells (high isolation purity/specificity), (iii) perform this analysis sufficiently fast, and (iv) handle rather large volumes of sample (high system throughput) (9).

CTCs have been distinguished based on size, deformability and density (22–24). However, these physical parameters may significantly vary throughout the CTC population and thus also lead to significant overlap with normal cells. The majority of platforms, including the first commercially available CTC diagnostic system (Cellsearch, Veridex), therefore identifies CTCs based primarily on their specific protein marker expression such as epithelial cell adhesion molecule (EpCAM) via immunoaffinity binding (14) or immunomagnetic isolation (25–30). In addition, negative markers, biophysical characteristics (e.g. size and deformability) and morphological analysis of CTC candidates are commonly employed.

Here we present work on a novel centrifugal microfluidic system that can magnetically isolate, enumerate, and detect rare cells on a low-complexity platform which is highly amenable to PoC diagnostics. Our previous work demonstrated continuous separation of magnetic beads of varying sizes from a large background of cell-mimicking beads (31) and HIV relevant cell separation of CD4-positive cells (32). We have now critically advanced the earlier technology to isolate much lower, biologically relevant concentrations of CTC-mimicking, cultured MCF7 breast cancer cells (from cell lines) spiked into a whole blood sample. We use paramagnetic, antibody-coated microbeads which target the MCF7 cells by binding to the EpCAM epitope expressed on these cells with very high specificity. Our continuous-mode, centrifugo-magnetophoretic system can therefore separate the input sample into its three superordinate constituents: (red and white) blood cells, magnetically tagged target (cancer) cells and excess unbound magnetic beads.

A unique feature of this multiforce separation is the removal of unbound paramagnetic beads from tagged magnetic cells based upon the synergistic interplay of magnetic and centrifugal fields with the size-dependent Stokes drag. While many platforms (32,33) have used magnetic separation, they lack the ability to remove unbound magnetic beads from isolated tagged target cells. This is because such a purification, e.g. through integrated size filtration, tends to be prone to clogging and unspecific trapping, and may thus lead to the loss of scarce target cells which would be prohibitive for rare cell detection. Our filter-less, flow-less sedimentation-driven system presented here, by design, eliminates this critical flaw. Through the continuous sedimentation scheme, we also mitigate the risk of cell damage due to vigorous snapping of beads against the vessel wall and the risk of collective pull of entrapped target cells by the abundant background population into the waste; these parasitic loss mechanisms are deemed prevalent in common batch-mode magnetostatic separations.

Alongside presenting, for the first time, isolation of EpCAM positive cancer cells in biologically relevant concentrations using continuous centrifugo-magnetophoresis, we also demonstrate a proof-of-concept of a simple, bight-field method to quantitate the number of isolated cells based on their packing volume in the capture chamber. This technique is similar to established packed-cell-volume (PCV) haematocrit measurement (34) and other diagnostics platforms (7).

Working Principle

In our stopped-flow, continuous sedimentation centrifugo-magnetophoresis (i.e. particle sedimentation

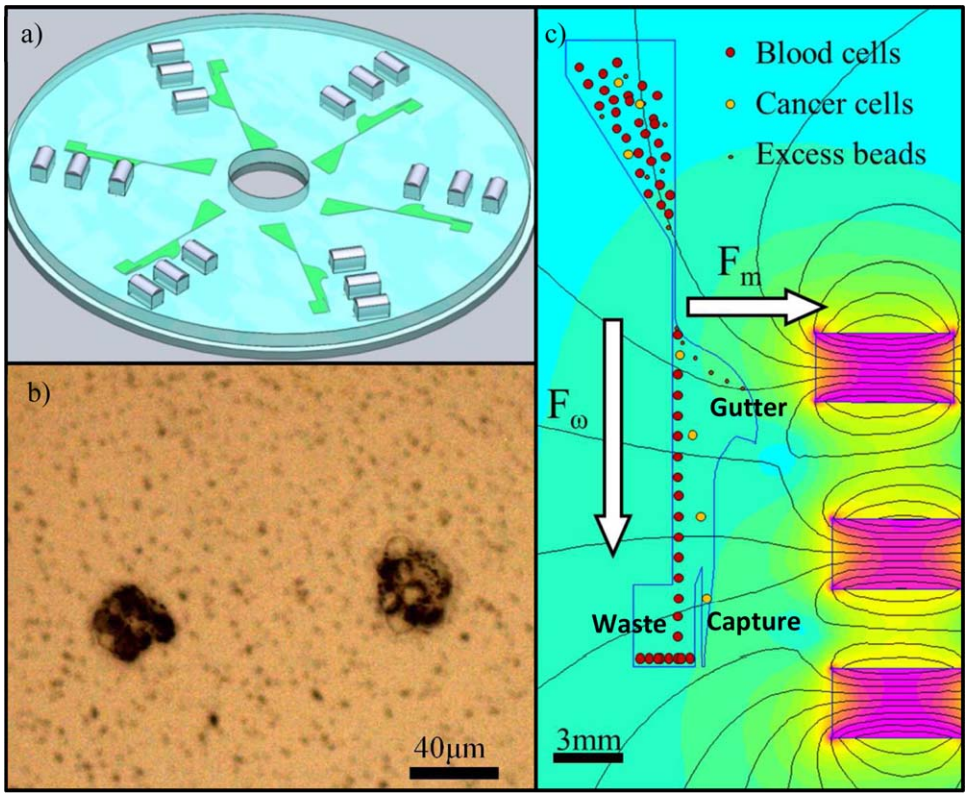

Figure 1. **a**) Schematic of the polymeric "lab-on-a-disc" with microfluidic channels, visible in green, and magnets as silver cylinders. **b**) Bright-field microscope image of two clusters of MCF7 cells tagged with paramagnetic beads (background beads are visible as dark specks). **c**) Magnetic field simulation of one of the green chambers from (a), with trajectories for blood cells, magnetically tagged (cancer) cells and excess magnetic beads. The directions of the centrifugal and magnetic fields are also indicated. Blood cells, excess beads, and cancer cells are routed to the blood waste ("waste"), bead waste ("gutter"), and target cell capture chamber ("capture"), respectively. Direction of rotation is CCW. [Color figure can be viewed in the online issue, which is available at wileyonlinelibrary.com.]

through a stationary liquid on a centrifugal platform with magnetic separation), the three forces governing the path of the particles through the system are the centrifugal force F_ω, the essentially lateral magnetic force F_m, and the hydrodynamic Stokes drag F_s (Fig. 1) (31). Nonmagnetic background blood cells will only experience the radial centrifugal force F_ω and the counteracting Stokes drag F_s to sediment on a straight path toward the peripheral edge of the disc. Concurrently, magnetic particles will additionally experience the lateral magnetic field F_m, and thus deflect from the main stream.

The separation between unbound magnetic beads and the magnetically tagged cancer cells (Fig. 1c) is primarily governed by the differences of (the densities of) their magnetic momenta (31); the bulk magnetized beads possess a notably larger mean magnetic momentum than the much larger cell/bead hybrids which only exhibit a magnetization on the surface of their biological core. The resulting differential in lateral magnetic deflection is enhanced by the steep increase of field gradient toward the co-rotating magnet, which thus amplifies the spatial separation compared with a (hypothetical) uniform field.

The two other factors, the centrifugal field and the viscous Stokes drag, are significantly smaller in magnitude and do not directly alter the deflection of the particle, i.e. the principal discriminator of our spatial separation technique. Instead, the interplay of these two counteracting forces mainly impacts the (radial) speed of sedimentation, which is only indirectly resolved by our technique through the residence time of the particles within the impact zone of magnetic deflection. However, the density differences between our types of bioparticles are significantly less pronounced than the differences in their magnetization, so the centrifugal field only constitutes a secondary effect in our separation mechanism.

Our stopped-flow centrifugo-magnetophoresis therefore drives a central stream of copious background cells into the radially aligned, main waste chamber (labeled "waste" in Fig. 1c). The most strongly magnetized, free beads are vigorously removed into a laterally aligned "gutter" chamber (labeled "gutter" in Fig. 1c). Finally, the less magnetized hybrids of the target cells with the bead-tags are routed closer to the main sedimentation direction into a slightly displaced, small detection chamber (labeled "capture" in Fig. 1c). Direction of rotation is counter-clockwise (CCW), which means any corialis effects will keep particles against the left-hand wall (Fig. 1c). Due to the low speed of sedimentation of the particles in stopped-flow mode, the impact of the Coriolis force was found to be negligible, but the sense of spinning direction was chosen as a precaution anyway.

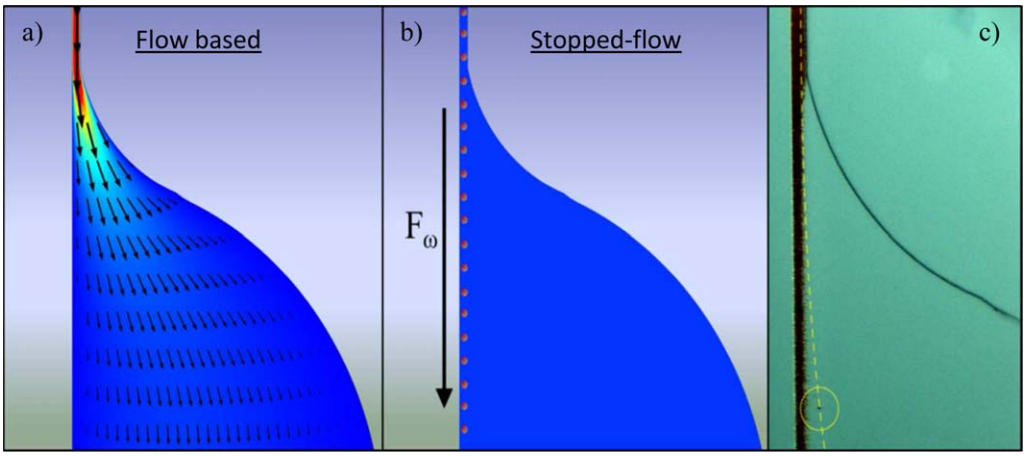

Figure 2. **a**) In a flow based system, any particles entering a wide chamber will follow the expanding streamlines and fill the whole structure. The Comsol Multiphysics simulation indicates the velocity field in such a flow-based chamber. **b**) In a stopped-flow, centrifugal sedimentation based system, particles entering a wide chamber will continue on their radial trajectory unless deflected by another force. **c**) Image obtained of bulk blood cells traveling radially outward while a magnetically tagged cancer cell is additionally deflected by a laterally placed magnet. The yellow line shows the path taken by the tagged cancer cell. (Video of separation can be found in Supporting Information.) [Color figure can be viewed in the online issue, which is available at wileyonlinelibrary.com.]

In this way our design provides a low-stress, threefold spatial separation of background blood cells, magnetically tagged cancer cells and excess tagging beads. Compared with standard, batch-mode immunomagnetic separation with a simple magnet, our continuous, sedimentation-driven system separates the latter two magnetic particles without the error-prone size filtration. Furthermore, the novel, stopped-flow mode inherently eliminates flow-field instabilities which tend to compromise resolution. Also, magnetostatic, batch-mode immunoseparation often leads to collective entrapment of rare target cells in a cohort of background cells. This loss mechanism is suppressed through the radially stretched distribution of the population of suspended cells through the continuous sedimentation mode.

Materials and Methods

Disc Manufacture

The manufacture of the microfluidic discs was based on the design from the author's previously published work (31). In brief, the discs were formed from polydimethylsiloxane (PDMS) (Sylgard 184, Dow Corning; #101697, Farnell, UK) by standard soft lithography methods (31) from a design drawn with AutoCAD (Autodesk, Inc., CA). A 100-μm thick dry-film photoresist (DuPont, NC) was hot-roll laminated onto a 4" silicon wafer, lithographically structured by UV exposure and developed according to the manufacturer's instructions. The dry film structures left on the wafer define the PDMS casted channels. The millimetre-scale indentations for magnet positioning (Fig. 3) were engineered with a three-dimensional-printed polymer mould (uPrint, Stratasys Ltd., MN) and aligned via guide pins to create highly reproducible discs with both, micro- and macrofeatures. After the PDMS had been poured into the mould and hardened in the oven (1 hr at 70°C), the discs were assembled and then placed for 1 h into a vacuum chamber to allowing subsequent, degas-driven priming (35) with buffer (phosphate buffered saline [PBS] with 10% EDTA and 1% casein). The magnets (S-03–06-N, Supermagnete, Germany) were then placed into the pre-moulded voids on the PDMS disc.

The Centrifugal Spin-Stand

The microfluidic disc is then loaded with sample and placed onto the custom designed centrifugal spin-stand (36) featuring a servo motor (4490 series, Faulhaber, DE), a CCD camera (Sensicam series, PCO, DE) connected to an optical imaging system (Navitar, NY), and a strobe light all synchronised via a PC (Dell). The system records one image per rotation, giving the user a live feed of the cells and microparticles as they sedimented through the microfluidic chambers. This provided detailed trajectory information and real-time counting of target cells, even during high-speed rotation.

Bead and Cell Binding

The basic separation mechanism here presented is dependent on specific binding of the 4.5 μm magnetic microbeads to the target cells of interest (Fig. 1c) (Dynabeads® Epithelial Enrich, Invitrogen Inc.). The Dynabeads were diluted 80-fold from stock and incubated at a 1:1 volume ratio with MCF7 cells spiked. All culture reagents were obtained from Sigma-Aldrich (MO) unless otherwise stated. MCF7 cells (DSMZ, Braunschweig, Germany) were cultured in 75 cm^3 flasks in DMEM media, supplemented with 10% uninactivated fetal bovine serum (FBS), 100 U/ml penicillin and 100 μg/ml streptomycin. Cultures were maintained at 37°C with 5% CO_2. Cells were harvested by incubation in 5 ml 0.25% trypsin/0.1% EDTA at 37°C for 5 min followed by neutralization with 5 ml culture medium. Cells were centrifuged at 300*g* for 4 min and resuspended in culture medium. Where indicated, live cells were fluorescently labeled with NucBlue™ Live Cell Stain (Life Technologies, CA) according to manufactures instructions. Whole blood, MCF7 cells and Dynabeads were incubated in a capped 2 ml tube on a rotator for approximately 10 min at

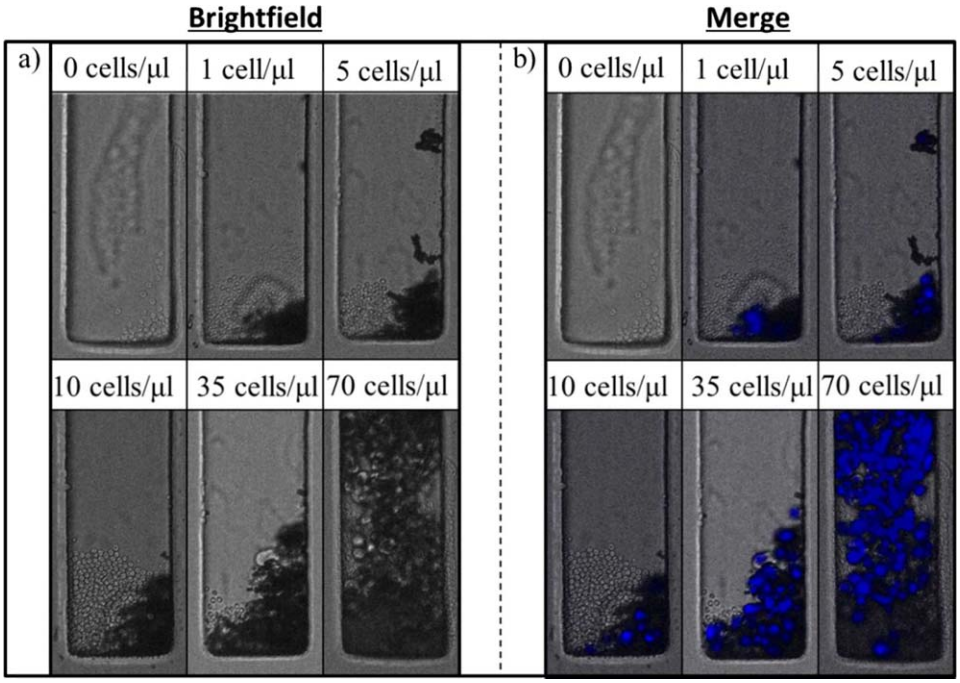

Figure 3. **a**) Bright-field image showing the magnetically tagged MCF7 cells in the capture chamber. This method was used for counting the dark pixels (tagged MCF7s) with the freeware ImageJ software (Fig. 4). **b**) Fluorescent merge image displaying the same magnetically tagged and NucBlue stained MCF7 cells in the capture chamber. This method was used to enumerate the amount of MCF7 cells present in the entire system, including any cells which did not reach the capture chamber (not shown). Chamber width: 150 μm. [Color figure can be viewed in the online issue, which is available at wileyonlinelibrary.com.]

room temperature. It was noted that substantial MCF7-cell-to-bead binding was observed within less than 5 min.

Experimental Results

Centrifugo-Magnetophoresis

Following incubation of the sample with magnetic beads (cf. Materials and Methods section), a 3 µl aliquot was loaded into each of the six chambers of the prepared microfluidic disc, providing a total volume of 18 μl. This sample of whole blood, tagged MCF7 cells and excess beads was then sedimented through the system by rotating the disc at a rate of 17 Hz (55 *g* at edge of disc). When viewed using a zoomed real-time video stream of the microfluidic chambers, within 10 s the first of the tagged MCF7 cells exit the focusing channel and are then deflected by the magnetic field into the separation chamber (Fig. 2c, also see video in Supporting Information). Within 1 min the MCF7 target cells are routed to their designated capture area (Fig. 3). The remainder of the particles (untargeted red and white blood cells, beads, and the remaining tagged cells) continue to sediment down the chamber to their respective capture areas (Fig. 1c); within 10 min the separation is completed. As shown in Figure 3, the centrifugo-magnetic stopped-flow system very accurately and reproducibly separates a very small number of target cancer cells from a background of a whole blood (as low as 1 cell/μl). Furthermore, the system can also very efficiently segregate the unbound background beads without error-prone steps such as size filtration. This removal of the unbound beads is of critical importance for the quantitation of the captured cells, as, otherwise, their presence in the target chamber would influence the level of packing measured.

Detection and Quantification

In order to engineer a low-cost and easy to use system, we obviated the need for any complex procedure and costly fluorescence imaging. Unlike many other published instrumentation (17,18) the specificity of detection in our system is not based on the binding of a specific fluorescent antibody, but rather on the specificity of the magnetic beads to the target cells of interest. As these cells are isolated from the background sample, and specifically directed to a dedicated detection locus, our here presented detection technique is based simply on analyzing the extent of occupation of this locus using bright-field imaging (Fig. 3a). The dark areas shown represent clusters of target cells surrounded with magnetic beads which are tightly packed by the centrifugal field. The darkness of the filling arises from the bead tags, and this facilitates simple image processing to quantify the extent of packing.

The surface area of the pack was found to be directly proportional to the (predefined) concentration of tagged cells in our spiked sample (Fig. 4). In order to quantify the exact number present for calibration purposes we fluorescently labeled the MCF7 cells with NucBlue dye beforehand (Fig. 3b). Note that for the later analysis and quantification, only the bright-field images were used.

We analyzed the bright-field images of the target cell capture chambers of all structures on the disc. Due to the high contrast of the cell/bead pack with respect to the background in

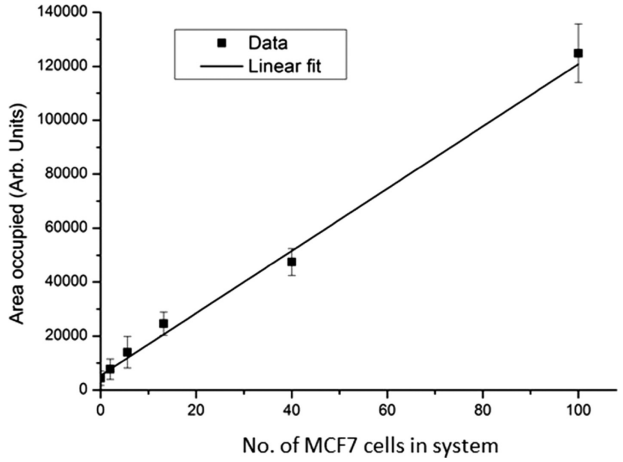

Figure 4. The area of the capture chamber occupied by dark pixels was calculated on ImageJ software and plotted against the total number (determined by fluorescent tagging) of MCF7 cells in the sample, giving a very close linear fit ($R^2 = 0.98$ and $n = 5$). This standard curve gives a baseline calibration to determine the concentrations of target cells present based on determination of the dark area.

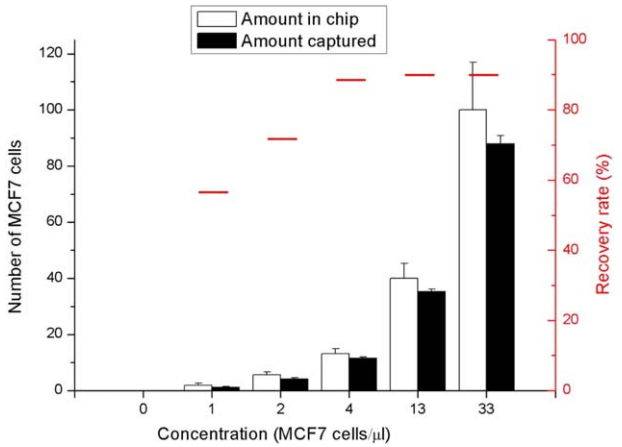

Figure 5. The total amount of MCF7 cells present in the chip is indicated in white, while the total number captured successfully is indicated in black. The mean recovery rate is 80% ($n = 5$), peaking at 88% at the highest concentration (indicated in red). [Color figure can be viewed in the online issue, which is available at wileyonlinelibrary.com.]

the capture chambers, a straight-forward method as part of the freeware image analysis software ImageJ (ImageJ, U.S. National Institutes of Health, MD) could be employed to enumerate the number of dark pixels in a predefined region of interest, and thus measure the extent of packing within each sample. A more indepth explanation of the image analysis is given in the Supporting Information. In brief, the background signal defined a threshold value and the image was converted to an 8-bit binary picture. The histogram could then be adjusted to provide the maximum contrast between the dark bead/cell clusters and the bright background. This gave a clear count of only the black pixels and widely suppressed noise from untagged blood cells or other stray particles. A set of six discs, with each running five identical samples, was analyzed using this method.

The total amount of MCF7 cells present in each of the whole blood tests, and the corresponding area calculated by the dark packing fraction method are shown in Figure 4. The correlation between packing area and known input is demonstrated by the standard curve of the graph. These estimated values correlated directly with the actual values shown in Figure 5, while the analysis strategy successfully identified the "healthy" sample (i.e. zero cancer cells) and also correctly assigned the values to the increasing concentrations of cancer-cell spiked samples that were as low as a single MCF7 cell per μl of whole blood sample. The capture efficiency, i.e. the ratio between the number of cancer cells retrieved after centrifugo-magnetic purification versus the total number of cancer cells introduced into the chip, is 80% on average, peaking at 88% for the highest concentration.

Discussion

We have presented the centrifugo-magnetophoretic purification and bright-field based quantification of rare cells from whole blood. A test on a total 18 µl of sample rapidly completes within 10 min on our lab-on-a-disc system; the first target cells are even detected in less than 1 min, which might be beneficial if the sheer presence of the diagnostic target cell was relevant (e.g. in the case of circulating tumour cells). The mean recovery ratio of the target cells was 80%, peaking at 88% toward higher concentrations. The target cell population can be quantified by a low-cost, bight-field opto-mechanical setup incorporating a spindle motor and a CCD-based readout akin to an optical disc drive like a CD or DVD player. We also note that this system could detect cells at a much lower concentration than here presented if the sample was purified and concentrated before the centrifugo-magnetophoretic procedure, e.g. by band extraction of the buffy coat or lysis of the erythrocytes. It is also worth noting that while EpCAM was used in these particular experiments, any target (or combination of targets) can be used through adoption of widely recognized bead technologies and bead-binding chemistries. Our system may thus be readily advanced to a compact, rapid, accurate, and fully automated sample-to-answer (rare) cell counter for point-of-care diagnostics.

Acknowledgments

The authors thank B. Bulfin for his assistance on flow simulations.

Literature Cited

1. Ducrée J, Haeberle S, Lutz S, Pausch S, Stetten F Von Zengerle R. The centrifugal microfluidic Bio-Disk platform. J Micromech Microeng 2007;17:S103–S115.
2. Gorkin R, Park J, Siegrist J, Amasia M, Lee BS, Park J-M, Kim J, Kim H, Madou M, Cho Y-K. Centrifugal microfluidics for biomedical applications. Lab Chip 2010;10:1758–1773.
3. Park J, Sunkara V, Kim T-H, Hwang H, Cho Y-K. Lab-on-a-disc for fully integrated multiplex immunoassays. Anal Chem 2012;84:2133–2140.
4. Burger R, Ducrée J. Handling and analysis of cells and bioparticles on centrifugal microfluidic platforms. Expert Rev Mol Diagn 2012;12:407–421.
5. Burger R, Kirby D, Glynn M, Nwankire C, O'Sullivan M, Siegrist J, Kinahan D, Aguirre G, Kijanka G, Gorkin RA, et al. Centrifugal microfluidics for cell analysis. Curr Opin Chem Biol 2012:1–6.
6. Potyrailo RA, Morris WG, Leach AM, Sivavec TM, Wisnudel MB, Boyette S. Analog signal acquisition from computer optical disk drives for quantitative chemical sensing. Anal Chem 2006;78:5893–5899.

7. Glynn MT, Kinahan DJ, Ducrée J. CD4 counting technologies for HIV therapy monitoring in resource-poor settings–state-of-the-art and emerging microtechnologies. Lab Chip 2013;13:2731–2748.
8. Arya SK, Lim B, Rahman ARA. Enrichment, detection and clinical significance of circulating tumor cells. Lab Chip 2013:1995–2027.
9. Li P, Stratton ZS, Dao M, Ritz J, Huang TJ. Probing circulating tumor cells in microfluidics. Lab Chip 2013;13:602–609.
10. Lianidou ES, Markou A. Circulating tumor cells in breast cancer: Detection systems, molecular characterization, and future challenges. Clin Chem 2011;57:1242–1255.
11. Cristofanilli M. Circulating tumor cells, disease progression, and survival in metastatic breast cancer. Semin Oncol 2006;33:S9–S14.
12. Cho EH, Wendel M, Luttgen M, Yoshioka C, Marrinucci D, Lazar D, Schram E, Nieva J, Bazhenova L, Morgan A, et al. Characterization of circulating tumor cell aggregates identified in patients with epithelial tumors. Phys Biol 2012;9: 016001.
13. Scher HI, Jia X, de Bono JS, Fleisher M, Pienta KJ, Raghavan D, Heller G. Circulating tumour cells as prognostic markers in progressive, castration-resistant prostate cancer: A reanalysis of IMMC38 trial data. Lancet Oncol 2009;10:233–239.
14. Nagrath S, Sequist LV, Maheswaran S, Bell DW, Irimia D, Ulkus L, Smith MR, Kwak EL, Digumarthy S, Muzikansky A, et al. Isolation of rare circulating tumour cells in cancer patients by microchip technology. Nature 2007;450:1235–1239.
15. Park J, Kim M, Moon H, Yoo C, Park D, Kim Y, Han K, Lee J, Oh J, Kim S, et al. Fully automated circulating tumor cell isolation platform with large-volume capacity based on lab-on-a-disc. Anal Chem 2014;86:3735–3742.
16. Mocellin S, Keilholz U, Rossi CR, Nitti D. Circulating tumor cells: The "leukemic phase" of solid cancers. Trends Mol Med 2006;12:130–139.
17. Autebert J, Coudert B, Bidard F-C, Pierga J-Y, Descroix S, Malaquin L, Viovy J-L. Microfluidic: An innovative tool for efficient cell sorting. Methods 2012;57:297–307.
18. Zhang Z, Nagrath S. Microfluidics and cancer: Are we there yet? Biomed Microdevices 2013;15:595–609.
19. Chen J, Li J, Sun Y. Microfluidic approaches for cancer cell detection, characterization, and separation. Lab Chip 2012;12:1753–1767.
20. Cima I, Wen Yee C, Iliescu FS, Min Phyo W, Hon Lim K, Iliescu C, Han Tan M. Label-free isolation of circulating tumor cells in microfluidic devices: Current research and perspectives. Biomicrofluidics 2013;7:011810.
21. Stott SL, Hsu C-H, Tsukrov DI, Yu M, Miyamoto DT, Waltman BA, Rothenberg SM, Shah AM, Smas ME, Korir GK, et al. Isolation of circulating tumor cells using a microvortex-generating herringbone-chip. Proc Natl Acad Sci USA 2010;107:18392–18397.
22. Müller V, Stahmann N, Riethdorf S, Goetz A, Ja F, Pantel K. Circulating tumor cells in breast cancer: Correlation to bone marrow micrometastases, heterogeneous response to systemic therapy and low proliferative activity. Clin Cancer Res 2005: 3678–3685.
23. Vona G, Sabile A, Louha M, Sitruk V, Romana S, Franco D, Pazzagli M, Vekemans M, Lacour B, Paterlini-Bre P. Isolation by size of epithelial tumor cells Am J Pathol 2000;156:57–63.
24. Di Carlo D. Inertial microfluidics. Lab Chip 2009;9:3038–3046.
25. Issadore D, Chung J, Shao H, Liong M, Ghazani AA, Castro CM, Weissleder R, Lee H. Ultrasensitive clinical enumeration of rare cells ex vivo using a micro-hall detector. Sci Transl Med 2012;4:141ra92.
26. Breukers C, Tibbe AGJ, Ymeti A, Li X, Terstappen LWMM, Greve J. A single platform image cytometer for resource-poor settings to monitor disease progression in HIV infection. Cytometry Part A J Int Soc Anal Cytol 2007;142A:132–142.
27. Pamme N. On-chip bioanalysis with magnetic particles. Curr Opin Chem Biol 2012; 16:436–443.
28. Hoshino K, Huang Y-Y, Lane N, Huebschman M, Uhr JW, Frenkel EP, Zhang X. Microchip-based immunomagnetic detection of circulating tumor cells. Lab Chip 2011;11:3449–3457.
29. Kang JH, Krause S, Tobin H, Mammoto A, Kanapathipillai M, Ingber DE. A combined micromagnetic-microfluidic device for rapid capture and culture of rare circulating tumor cells. Lab Chip 2012;12:2175–2181.
30. Helou M, Reisbeck M, Tedde SF, Richter L, Bär L, Bosch JJ, Stauber RH, Quandt E, Hayden O. Time-of-flight magnetic flow cytometry in whole blood with integrated sample preparation. Lab Chip 2013;13:1035–1038.
31. Kirby D, Siegrist J, Kijanka G, Zavattoni L, Sheils O, O'Leary J, Burger R, Ducrée J. Centrifugo-magnetophoretic particle separation. Microfluid Nanofluidics 2012;13: 899–908.
32. Glynn M, Kirby D, Chung D, Kinahan DJ, Kijanka G, Ducrée J. Centrifugo-magnetophoretic purification of CD4+ cells from whole blood toward future HIV/AIDS point-of-care applications. J Lab Autom 2013;19:285–296.
33. Darabi J, Guo C. On-chip magnetophoretic isolation of CD4 + T cells from blood. Biomicrofluidics 2013;7:54106.
34. Galanzha EI, Shashkov E V, Kelly T, Kim J-W, Yang L, Zharov VP. In vivo magnetic enrichment and multiplex photoacoustic detection of circulating tumour cells. Nat Nanotechnol 2009;4:855–860.
35. Riegger L, Grumann M, Steigert J, Lutz S, Steinert CP, Mueller C, Viertel J, Prucker O, Rühe J, Zengerle R, et al. Single-step centrifugal hematocrit determination on a 10-$ processing device. Biomed Microdevices 2007;9:795–799.
36. Hosokawa K, Sato K, Ichikawa N, Maeda M. Power-free poly(dimethylsiloxane) microfluidic devices for gold nanoparticle-based DNA analysis. Lab Chip 2004;4: 181–185.
37. Grumann M, Brenner T, Beer C, Zengerle R, Ducréé J. Visualization of flow patterning in high-speed centrifugal microfluidics. Rev Sci Instrum 2005;76:025101.